Regenerative Therapy 27 (2024) 342–353

Contents lists available at ScienceDirect

Regenerative Therapy

journal homepage: http://www.elsevier.com/locate/reth

Original Article

Recombinant human annexin A5 accelerates diabetic wounds healing by regulating skin inflammation

Bijun Kang [1], Zhuoxuan Jia [1], Yushan Dong, Wei Li**, Wenjie Zhang*

Department of Plastic and Reconstructive Surgery, Shanghai 9th People's Hospital, Shanghai Jiao Tong University School of Medicine, Shanghai Key Laboratory of Tissue Engineering, National Tissue Engineering Center of China, 639 ZhiZaoJu Road, Shanghai 200011, China

ARTICLE INFO

Article history:
Received 19 January 2024
Received in revised form
3 March 2024
Accepted 15 March 2024

Keywords:
Annexin A5
Macrophage
Diabetic wound healing
Skin inflammation
CEFFE

ABSTRACT

Background: One of the key obstacles to the healing of diabetic wound is the persistence of active inflammation. We previously demonstrated the potential of cell-free fat extract (CEFFE) to promote the healing of diabetic wounds, and annexin A5 (A5) is a crucial anti-inflammatory protein within CEFFE. This study aimed to evaluate the therapeutic potential of A5 in diabetic wounds.

Methods: A5 was loaded into GelMA hydrogels and applied to skin wounds of diabetic mice *in vivo*. The diabetic wounds with the treatment of GelMA-A5 were observed for 14 days and evaluated by histological analysis. Accessment of inflammation regulation were conducted through anti-CD68 staining, anti-CD86 and anti-CD206 staining, and qRT-PCR of wound tissue. In presence of A5, macrophages stimulated by lipopolysaccharide (LPS) *in vitro*, and detected through qRT-PCR, flow cytometry, and immunocytofluorescence staining. Besides, epithelial cells were co-cultured with A5 for epithelialization regulation by CCK-8 assay and cell migration assay.

Results: A5 could promote diabetic wound healing and regulate inflammations by promoting the transition of macrophages from M1 to M2 phenotype. *In vitro* experiments demonstrated that A5 exerted a significant effect on reducing pro-inflammatory factors and inhibiting the polarization of macrophages from M0 toward M1 phenotype. A5 significantly promoted the migration of epithelial cells.

Conclusion: Annexin A5 has a significant impact on the regulation of macrophage inflammation and promotion of epithelialization.

1. Introduction

Wound healing is a complex and dynamic process that involves the regulation of inflammation, angiogenesis, epithelialization and regeneration of the dermal extracellular matrix (ECM). Wound healing is generally divided into four consecutive stages: hemostasis, inflammation, proliferation, and tissue remodeling. Chronic wounds are characterized by delayed healing, prolonged inflammation, and impaired epithelialization. Diabetic wounds are the most common chronic wounds [1], with the core reasons for non-healing being the persistence of chronic inflammation and ischemia, reduced cell proliferation, and attenuated matrix synthesis [2]. Macrophages play crucial roles in wound healing. In the early stages of wound healing, monocytes and skin-resident macrophages are activated and polarized into M1-phenotype macrophages, which play a role in scavenging, phagocytosis, and the continued release of pro-inflammatory factors [3,4]. As macrophages transition from the pro-inflammatory M1 phenotype to the pro-repair M2 phenotype, the process of wound healing shifts from the inflammation phase to the proliferation phase, leading to a gradual subsidence of inflammation and the commencement of skin tissue regeneration and repair [5]. During the tissue remodeling phase of wound healing, macrophages secrete matrix metalloproteinases (MMPs) and tissue inhibitors of metalloproteinase (TIMPs), which participate in the regulation of the deposition and degradation of the dermal ECM, affecting tissue remodeling and scar formation [6,7]. In diabetic wounds, hyperactivation of M1

* Corresponding author.
** Corresponding author.
E-mail addresses: liweiboshi@163.com (W. Li), wenjieboshi@aliyun.com (W. Zhang).

Peer review under responsibility of the Japanese Society for Regenerative Medicine.

[1] Bijun Kang and Zhuoxuan Jia contributed equally to this work.

https://doi.org/10.1016/j.reth.2024.03.013

macrophages leads to prolonged chronic inflammation, which hinders wound healing.

Treatment of diabetic wounds has long been a significant challenge in clinical practice [8]. Recent advances in stem cell research have provided new treatment options [9]. Many studies have suggested that mesenchymal stem cells (MSCs) can promote the healing of diabetic wounds [10], which is thought to be associated with their paracrine effects [11,12]. Through the secretion of active factors, MSCs regulate inflammation, promote angiogenesis, enhance cell proliferation, and inhibit apoptosis [13]. However, stem cell therapy faces safety and stability challenages [14]. The development of drugs with diverse biological functions that can serve as stem cell substitutes is a crucial research focus. In a previous study, we demonstrated that cell-free fat extract (CEFFE) contains abundant bioactive proteins with various biological effects, including regulating inflammation, facilitating angiogenesis, and promoting cell proliferation and migration, all of which contributed to the healing of diabetic wounds [15,16]. CEFFE inhibits the expressions of pro-inflammatory factors, such as interleukin (IL)-1β, IL-6, inducible nitric-oxide synthase (iNOS) and tumor necrosis factor alpha (TNF-α), as well as promoting the expression of anti-inflammatory factors such as arginase 1(ARG-1), IL-10, CD206, and transforming growth factor beta (TGF-β), which directly regulates the transition of polarization of M1-phenotype macrophages into M2-phenotype macrophages [17].

However, CEFFE contains over 1700 types of bioactive proteins, making it a complex cell-free liquid mixture that does not meet the criteria of clearly defined pharmaceutical ingredients with controllable quality and the demands for large-scale industrial production. A solution to this challenge lies in the identification of the core components of CEFFE, and their subsequent synthesis using recombinant protein technology. Therefore, we conducted multiple rounds of CEFFE protein fractionation by protein chromatography and validated its anti-inflammatory effect. Finally, we identified a key protein, annexin A5 (A5), that is responsible for the anti-inflammatory effects of CEFFE (unpublished data). Annexin A5, a phospholipid-binding protein with a molecular weight of approximately 35.8 kDa, binds in a Ca^{2+}-dependent manner to negatively charged phospholipids on cell membranes [18,19]. When cell membranes are impaired, A5 binds to exposed externalized phosphatidylserine (PS) to form two-dimensional crystalline arrays, which are widely used for the detection of early apoptotic cells [20]. During the process of cell apoptosis, when PS is exposed on the outer membrane, it sends an 'eat me' signal that attracts phagocytes to engulf the cells. However, A5 can inhibit the engulfment of apoptotic cells by macrophages after binding to PS, thereby exerting an anti-inflammatory effect [21]. Clinical trials have demonstrated the safety of A5 in both healthy individuals (NCT04217629, NCT04850399) and patients with normal kidney function [22,23]. Additionally, a phase 2 trial is ongoing to evaluate the safety, pharmacokinetics and efficacy of A5 in patients with sepsis (NCT04898322). These clinical researches highlight the potential of A5 for clinical therapy and emphasize its anti-inflammatory property.

As chronic inflammation is a significant contributor to the non-healing of wounds, we hypothesized that A5 is a key component of CEFFE for treating non-healing wounds. Gelatin methacryloyl (GelMA) hydrogels, a photosensitive hydrogel with excellent biocompatibility, biodegradability, non-toxicity and non-immunogenicity, were suited to be widely utilized in tissue engineering and drug delivery [24]. In this study, A5 was loaded into GelMA hydrogels for the treatment of diabetic wound. Both *in vivo* and *in vitro* experiments about diabetic wound healing were to investigate the potential mechanisms of A5 treatment.

2. Materials and methods

2.1. Diabetic wound model and treatment

This study included 18 male BKS-*Lepr*^{em2cd479}/Gpt mice, aged 6–8 weeks, with a mean weight of 36.48 ± 1.44 g, purchased from GemPharmatech Company (Nanjing, China). The animals were housed under conditions that provided ample food and clean water at a suitable temperature and humidity with 12-h light–dark cycles. This study was approved by the Animal Care and Experiment Committee of Shanghai Jiaotong University School of Medicine and adhered to the recommendations of the National Research Council Guide for the Care and Use of Laboratory Animals.

To ensure that all of the mice were diabetic, the blood glucose levels in each animal were measured before the start of the experiment by Accu-Chek Active Blood Glucose Meter (Roche, Switzerland) and the mean blood glucose of the mice was 23.23 ± 5.99 mmol/L. The mice were then anesthetized using pentobarbital, and their dorsal skin was depilated. A full-thickness 8 mm skin wound was made by punch biopsy of the centrodorsal skin of each diabetic mouse, and the mice were then randomly divided into three groups (n = 6 per group): CTRL, GelMA, and GelMA-A5. The content of A5 in CEFFE is ranged from 5.34 μg/mL to 52.55 μg/mL, and 20 μg/mL annexin A5 was chosen to conduct the experiments.

GelMA and lithium phenyl-2,4,6-trimethylbenzoyl phosphinate (LAP) photoinitiator were purchased from Engineering for Life Co., Ltd. (Suzhou, China). A 0.25% LAP photoinitiator standard solution was mixed with a 5% GelMA solution. The hydrogel solution was passed through a 0.22 μm filter to ensure sterility. The prepared hydrogel solution was mixed with phosphate buffer saline (PBS) solution (GelMA-PBS hydrogel) or 40 μg/mL recombinant annexin A5 solution (GelMA-A5 hydrogel) in a 1:1 ratio (v:v). GelMA-PBS hydrogel solution was applied to the wounds in the mice of the GelMA group, while GelMA-A5 hydrogel solution was applied to the wounds in the mice of the GelMA-A5 group, with each application amounting to 80 μL. The hydrogel solution was immediately cross-linked by exposure to UV light at a wavelength of 405 nm for 15 s.

The wound healing was observed and photographed on days 0, 3, 7, 10, and 14 after wound occurrence, and the wound tissues were harvested on the 14th day. The wound area (%) was analyzed and quantified using Image J software (NIH) and calculated using the following formula.

$$\text{Wound area } (\%) = \frac{\text{Actual wound area}}{\text{Original wound area}} \times 100\%$$

2.2. Drug release of A5 from GelMA hydrogel

The GelMA-A5 hydrogel (500 μL) was cross-linked in Eppendorf tube. PBS (1 mL) as the release medium was add and the tubes was incubated at 37 °C. At the predetermined time points, 0.1 mL of supernatants were collected and 0.1 mL PBS solution were supplemented. The A5 content of collected supernatants were detected by Human Annexin A5 ELISA Kit (ab223863; Abcam, Cambridge, UK) at 450 nm using a microplate reader (SpectraMAX® 190, Molecular Devices, Sunnyvale, CA, USA).

$$\textit{Cumulative release } (\mu g / mL) = \frac{C_n V \pm \sum_{i+1}^{n-1} C_i V_i}{W}$$

2.3. Histological analysis

The wound tissues were fixed with 4% paraformaldehyde, dehydrated, and embedded in paraffin. Depending on the protocol, the tissue sections were stained by hematoxylin and eosin (H&E) or Masson's trichrome (Solarbio, Beijing, China). The sections were scanned and photographed with a Nikon Eclipse 90i digital camera and an optical microscope (Nikon, Tokyo, Japan).

2.4. Immunohistochemical staining

The wound tissue sections were subjected to immunohistochemical staining. Briefly, following antigen retrieval and permeabilization, sections were incubated with primary antibodies at 4 °C overnight and secondary antibodies at room temperature for 1 h. Finally, the DAB substrate solution was used to reveal the color of the antibody staining. The primary antibodies used in this study were rabbit monoclonal anti-CD68 (1:100; SC-20060; Santa Cruz, Texas, USA), anti-CD31 (1:1000; ab182981; Abcam, Cambridge, UK), and anti-PCNA (1:500; 60097-1-1 g; Proteintech, Wuhan, China). The secondary antibodies used were horseradish peroxidase-conjugated polymer anti-rabbit and anti-mouse antibodies (1:1000; Dako, Glostrup, Denmark). The sections were photographed with a Nikon Eclipse 90i digital camera and an optical microscope (Nikon, Tokyo, Japan). The immunohistochemical staining was analyzed with ImageJ software (NIH) to calculate the integrated optical density of anti-CD68-positive cells and epithelial anti-PCNA-positive cells. The capillary density was calculated as the number of anti-CD31-positive vessels. Three sections of each sample were analyzed.

2.5. Immunofluorescence staining of section

Immunofluorescence staining was performed on wound tissue sections and cells on coverslips. Following the routine steps of immunofluorescence staining, primary antibodies were incubated at 4 °C overnight, and secondary antibodies were incubated at room temperature for 1 h. DAPI staining solution (P0131; Beyotime, Shanghai, China) was used to stain the cell nuclei. The primary antibodies used were rabbit monoclonal anti-CD86 (1:200; 19589S; CST, USA) and anti-CD206 (1:400; 24595S; CST, USA). The secondary antibodies used were Alexa Fluor® 488-conjugated anti-mouse antibody (1:1000; 4412S; CST, USA) and Alexa Fluor® 594-conjugated anti-rabbit antibody (1:1000; 8889S; CST). The sections and coverslips were scanned and photographed with a Leica LAS X system and a confocal fluorescence microscope (Leica, Wetzlar, Germany) and then analyzed using ImageJ software (NIH) to calculate the fluorescence density (/mm2). Three sections of each sample were analyzed. ImageJ software was also used to analyze the fluorescence intensity.

2.6. Quantitative real-time PCR

Tissue and cellular mRNA were extracted using a Tissue RNA Purification Kit PLUS (EZB-RN001-plus; EZBioscience®, Roseville, USA) and an EZ-press RNA Purification Kit (B0004DP; EZBioscience®), respectively, according to the manufacturer's instructions. Following determination of the RNA concentration, 1 μg of the mRNA was reverse transcribed to cDNA using 4 × Reverse Transcription Master Mix (A0010CGQ; EZBioscience®). Quantitative real-time PCR (qRT-PCR) was performed using SYBR™ Green qPCR Master Mix (A0012-R2; EZBioscience®), primers, and cDNA. At least three technical replicates were analyzed for each sample. The results were calculated using the 2^(−ΔΔCt) method and are presented as the fold change relative to GAPDH gene expression. The primer sequences used for the qRT-PCR are shown in Supplementary Table 1.

2.7. Cell culture

Bone marrow mononuclear cells, obtained from the femur bone marrow of male C57BL/6 mice aged 4–6 weeks (Weitong Lihua, China), were cultured in dulbecco's modified eagle medium (DMEM) containing 20 ng/mL M-CSF, 10% fetal bovine serum, 100 U/mL penicillin, and 100 μg/mL streptomycin to induce primary M0-phenotype bone marrow-derived macrophages (BMDMs). After one week of cell culture, *in vitro* inflammatory models were induced using 1 ng/mL lipopolysaccharide (LPS), with the application of A5 at different concentrations of 0, 2.5, 5, and 10 μg/mL.

Human immortal keratinocytes (HaCaT) and human umbilical vascular endothelial cells (HUVECs) were purchased from the American Type Culture Collection (ATCC, Rockville, MD, USA). The HaCaTs and HUVECs were cultured in DMEM medium containing 10% fetal bovine serum, 100 U/mL penicillin, and 100 μg/mL streptomycin. Human dermal fibroblasts (HFBs) were isolated from skin tissues obtained from five donors (ages 6–10 years) undergoing routine circumcision at Shanghai 9th People's Hospital and the informed consent for HFBs isolation was obtained. After digestion with neutral protease and collagenase, dermal fibroblasts were cultured in DMEM containing 10% fetal bovine serum, 100 U/mL penicillin, and 100 μg/mL streptomycin. The experiments were conducted using HFBs during the first and third passages. The medium was changed every two days, and the cells were passaged and used for experiments when the cell density reached 90%. For the *in vitro* experiments, the cells cultured in the presence of A5 at 0, 2.5, 5, and 10 μg/mL. All cells were cultured in a humidified cell culture incubator at 37 °C with 5% CO2.

2.8. Flow cytometry

After culturing LPS-stimulated BMDMs in the presence of A5 at 0, 2.5, 5, and 10 μg/mL for 24 h, the cells were scraped from the culture plates, resuspended in cell staining buffer (420201; Biolegend, USA), and incubated on ice. FITC-*anti*-CD86 antibody (1:40; 105005; Biolegend, USA) was added and incubated for 30 min. After washing with cell staining buffer, the cells were detected by flow cytometry (Beckman Coulter), and the data were analyzed using FlowJo software (Becton, Dickinson & Company).

2.9. Cell counting kit 8 (CCK-8) assay

HaCaTs, HUVECs, or HFBs were seeded in 96-well plates at 3 × 103 cells per well. After they had adhered, the cells were cultured in the presence of A5 at 0, 2.5, 5, and 10 μg/mL. Cell proliferation was assessed on days 1, 2, and 3. Following removal of the culture medium, CCK-8 reagent diluted 10 times was added to each well (100 μL per well) and incubated at 37 °C for 2 h. The optical density (O.D.) was then measured at 450 nm using a microplate reader (SpectraMAX® 190, Molecular Devices, Sunnyvale, CA, USA). Relative O.D. values were calculated as follows:

Relative O.D. value = Experimental group O.D. value - Blank group O.D. value.

2.10. Cell migration assay

HaCaTs and HUVECs were seeded in 6-well plates at 2 × 105 cells per well. After reaching 90% confluence, a sterile 200 μL pipette tip was used to create a scratch in the center of each well. The cells were then cultured in the presence of A5 at different concentrations, and images of the cell migration in the same wound

area were captured at 0, 12, and 18 h using an optical microscope (Carl Zeiss, Oberkochen, Germany). The cell migration was analyzed using ImageJ software (NIH), and gap closure was calculated using the following formula:

$$\text{Gap closure}\ (\%) = \frac{\text{Original scratch area} - \text{Actual scratch area}}{\text{Original scratch area}} \times 100\%$$

2.11. Tube formation assay

Tube formation assay was conducted by using Matrigel® (356231; Corning, NY, USA). After 50 μL of Matrigel® per well had solidified in 96-well plates, the HUVECs were cultured in the presenc of 0, 2.5, 5, and 10 μg/mL A5. After 6 h, the cells were stained with calcein-AM solution (Yeason, Shanghai, China) and photographed using a fluorescence microscope (Carl Zeiss, Oberkochen, Germany). The tube formation was quantified using ImageJ software (NIH) to analyze the number of branch points (/mm2) and the mean tube length.

2.12. Statistical analysis

All of the data are presented as means ± the standard error of the mean (SEM). One-way analysis of variance was performed to determine statistically significant differences between groups. The statistical analyses were performed using GraphPad Software (GraphPad Software, Inc., La Jolla, CA, USA). Statistical significance was set at $P < 0.05$.

3. Results

3.1. A5 accelerated diabetic wound healing In vivo

To assess the effect of A5 on non-healing wounds, we applied a GelMA hydrogel containing A5 to the skin wounds of diabetic mice (Fig. 1a) and observed the process of wound healing on days 0, 3, 7, 10, and 14. The concentration of A5 released from GelMA-A5 hydrogel in PBS gradually increased with the incubation time prolonging, which demonstrated the property of GelMA hydrogel with drug sustained release (Fig. S1). In the early stages, the wounds in the untreated CTRL group exhibited an increased area due to tissue tension, whereas the wounds treated with hydrogel in the GelMA and GelMA-A5 groups effectively prevented tension (Fig. 1b and c). Over time, the wounds treated with A5 exhibited significantly accelerated healing compared with those of the CTRL group and demonstrated a notable advantage over the GelMA group. By the 14th day of treatment, the wound area (%) of CTRL, GelMA, GelMA-A5 group were 56.85% ± 3.84%, 28.83% ± 5.20% and 6.40% ± 4.32%, respectively (Fig. 1c). What is noteworthy is that the wounds treated with A5 exhibited were close to complete healing. These results indicated a significant role of A5 in accelerating diabetic wound healing.

3.2. A5 treatment accelerated diabetic wounds into the tissue remodeling phase

Histological changes in diabetic wounds on day 14 were observed by H&E and Masson's trichrome staining. Fig. 2 provided an overall wound tissue at low magnification, and highlighted the specific tissue regions at the wound ends and central area under high magnification. The sections stained with H&E staining in the CTRL group exhibited the wider discontinuous epidermis and incomplete skin structure, accompanied by significant infiltration of inflammatory cells. In comparison, the wounds in the GelMA group showed a smaller epidermis gap and the infiltration of inflammatory cells. In contrast, the wounds treated with A5 exhibited a continuous epidermis, intact skin structure in the central area, and reduced inflammatory cell infiltration (Fig. 2a). Masson's trichrome staining further revealed that the wound tissues in the CTRL groups displayed disordered collagen fiber structures with rich and dense collagen. And the wounds in the GelMA group showed less disordered collagen fiber structures, compared to the CTRL group. However, the A5-treated wounds exhibited a more orderly arrangement of collagen fibers, and the collagen deposition at the site of scar formation was reduced (Fig. 2b). These findings indicate that A5 treatment accelerated the transition of diabetic wounds into the tissue remodeling phase and had a positive impact on scar fibrosis.

3.3. A5 treatment promoted wound healing through regulating macrophages inflammation

We investigated whether A5 promoted diabetic wound healing by regulating inflammation. First, immunohistochemical anti-CD68 staining was performed on wound tissues to assess changes in infiltration of macrophages. The CTRL group exhibited a higher number of CD68-positive cells, the GelMA group exhibited reduced macrophage infiltration, and the GelMA-A5 group had the lowest macrophage population (Fig. 3a and b). These results suggested that A5 regulates macrophage inflammation in the skin. Furthermore, we used anti-CD86 and anti-CD206 immunofluorescence staining to label M1-phenotype and M2-phenotype macrophages, respectively. At the 14th day, the CTRL group exhibited a higher number of CD86-positive M1-phenotype macrophages, while the GelMA group showed a reduced number. But following A5 treatment, the GelMA-A5 group displayed the lowest count of the CD86-positive M1-phenotype macrophages (Fig. 3c and d). At the 14th day of diabetic wound healing, the CTRL group exhibited nearly absent CD206-positive M2-phenotype macrophages. When treated with GelMA-PBS gel, the wounds had an increase slightly of CD206-positive cells in GelMA group. But after A5 treatment, the GelMA-A5 group displayed a significant increase in M2-phenotype macrophages (Fig. 3c and e). The results of the tissue qRT-PCR indicated that the A5 treatment significantly decreased the gene expression levels of IL-1β and IL-6 which were secreted by M1-phenotype macrophages, and increased the expression levels of M2-phenotype macrophage-related genes such as TGF-β and CD206 (Fig. 3f). The results of immunofluorescence staining and qRT-PCR confirmed that A5 reduced the number of M1-phenotype macrophages and increased the number of M2-phenotype macrophages. These findings suggested that A5 regulated the inflammatory response of macrophages in diabetic wounds and promoted the transition from M1-phenotype to M2-phenotype macrophages.

3.4. No effect of A5 treatment on angiogenesis or epithelial proliferation

Angiogenesis and epithelialization are crucial for wound healing. The angiogenesis in diabetic wound healing is insufficient with reduced vascularity and capillary density [25]. To assess angiogenesis, immunohistochemical anti-CD31 staining was performed on wound tissues. There was no difference in the number of CD31-positive vessels among the three groups (Fig. 4a). The results suggested that A5 does not promote angiogenesis during diabetic wound healing. Regarding epithelial cell proliferation, anti-PCNA staining was performed on the wound tissues, and we observed no differences in the expression of PCNA in the epithelial layer

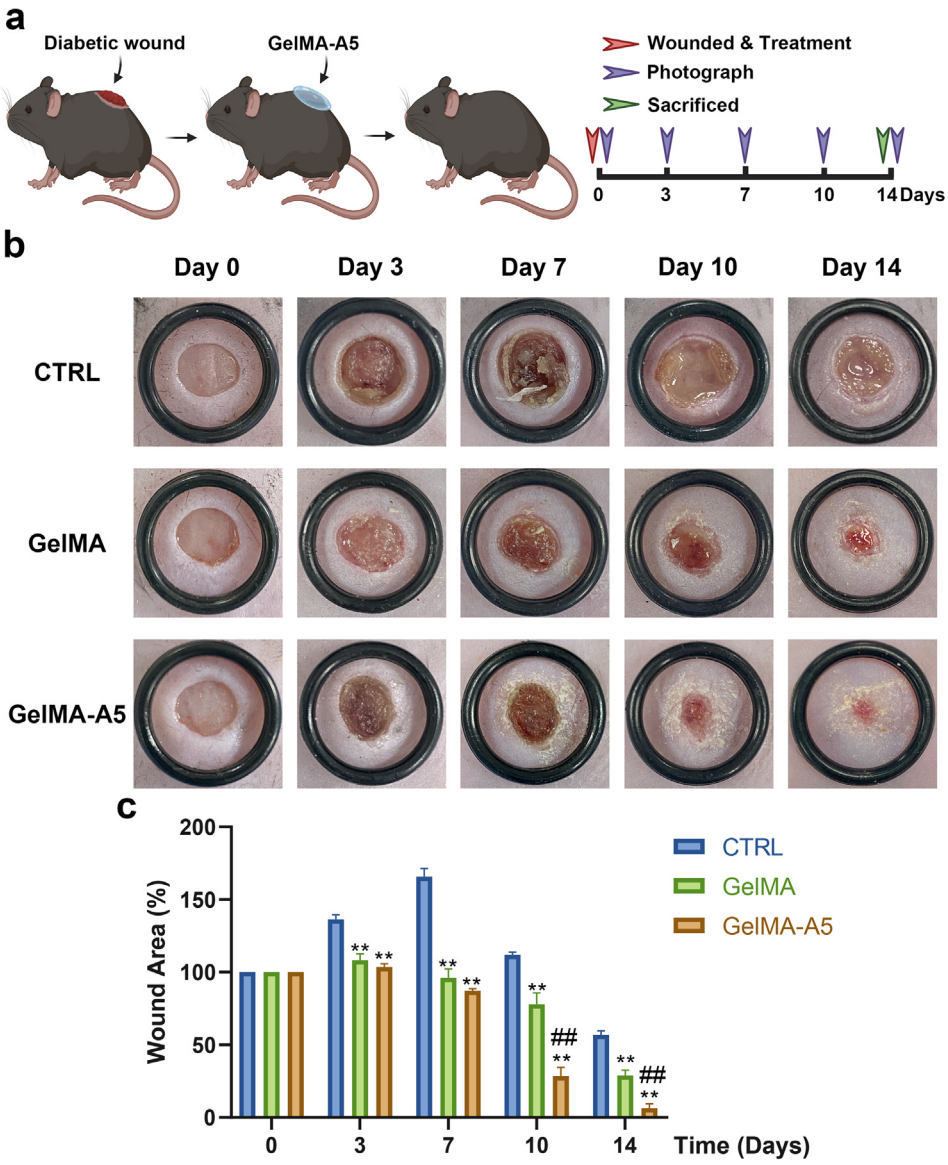

Fig. 1. A5 Accelerates Diabetic Wound Healing. A: Schematic representation of the animal experiment. B: Representative macroscopic photographs of wounds from the CTRL group, GelMA group, and GelMA-A5 group at days 0, 3, 7, 10, and 14. C: Percentage of wound area at days 0, 3, 7, 10, and 14. Data are presented as mean ± SEM, with n = 6 for each group. Statistical analyses were performed by comparing the GelMA and GelMA-A5 groups to the CTRL group, where *p < 0.05, **p < 0.05; and by comparing the GelMA and GelMA-A5 groups, where #p < 0.05, ##p < 0.05.

among the three groups (Fig. 4b). This finding implies that A5 did not affect the enhancement of epithelial cell proliferation during wound healing.

3.5. A5 regulated LPS-stimulated BMDM inflammation

We further confirmed the effect of A5 on macrophage inflammation by *in vitro* experiments. Using optical microscopy, compared with the M0-phenotype macrophages in the CTRL group, the LPS-stimulated macrophages exhibited evident morphological changes, including flattening into round and pancake-like shapes. However, macrophages cultured in the presence of A5 closely resembled those in the CTRL group (Fig. 5a). The results of the qRT-PCR showed that stimulation with LPS led to upregulation of pro-inflammatory cytokines (IL-1β, IL-6, and TNF-α), which are characteristic of M1-phenotype macrophages, while A5 treatment inhibited their upregulation. We found that A5 did not affect the expression of the anti-inflammatory factor ARG-1, which is characteristic of M2-phenotype macrophages (Fig. 5b). Flow cytometry assessment of anti-CD86 staining of the M1-phenotype macrophage marker revealed an increase in CD86-positive cells after stimulation with LPS, whereas A5-treated macrophages exhibited a decrease in CD86-positive cells (Fig. 5c and d). The results of immunofluorescence anti-CD86 staining were consistent with the flow cytometry findings (Fig. 5e). Collectively, these results suggest that A5 suppresses LPS-stimulated polarization of macrophages toward the M1 phenotype.

3.6. A5 promoted cell migration on HaCaTs

In *in vitro* experiments, HaCaTs were cultured in the presence of A5. Observation of HaCaTs over three days revealed no significant difference in cell proliferation between the group cultured in the presence of A5 and the CTRL group (Fig. 6a). However, in the cell

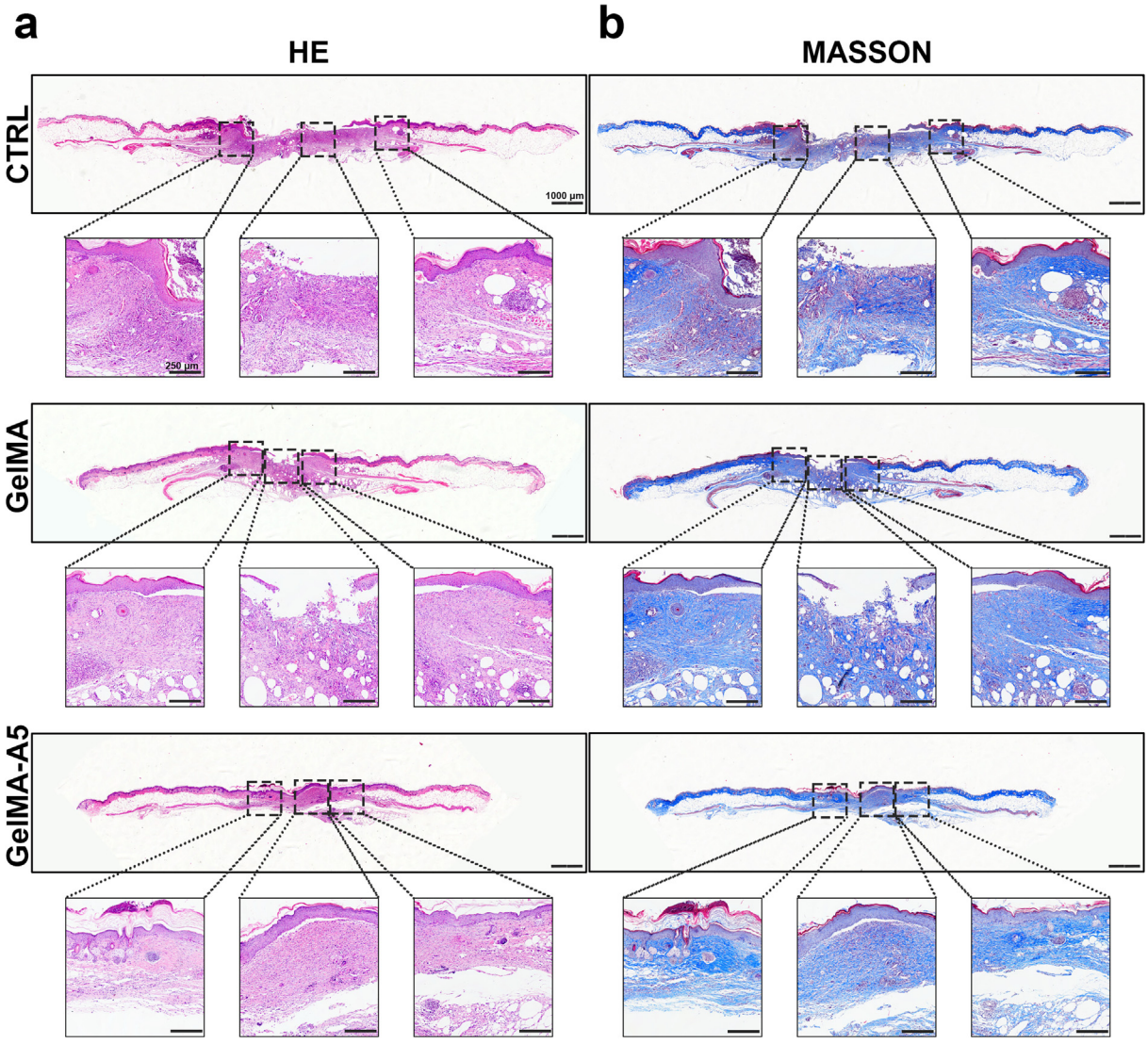

Fig. 2. Histological Changes in Diabetic Wounds Following Treatment of A5 On the 14th Day. A: HE staining of the CTRL group, GelMA group, and GelMA-A5 group. B: Masson's trichrome staining of the CTRL group, GelMA group, and GelMA-A5 group. The scale bar for the full wound tissue display is 1000 μm, and the scale bar for the local wound tissue display is 250 μm.

migration assay, compared to the 0-h scratch, a significant shrinkage of the scratch was observed in cells treated with A5 for 12 h. The promotion of cell migration was more apparent at A5 concentrations of 1.25 μg/mL and 2.5 μg/mL (Fig. 6b and c). These results indicate that A5 promotes epithelial cell migration without affecting cell proliferation, thereby contributing to epithelialization during wound healing.

3.7. A5 had No effect on dermal fibroblasts

To investigate the role of A5 in regeneration of the dermal ECM, fibroblasts were cultured in the presence of various concentrations of A5. Assessment of HFBs over three days using the CCK-8 assay revealed no significant difference in cell proliferation between A5-treated HFBs and the CTRL group (Fig. S2a). The qRT-PCR results indicated that the expression of type I collagen, type III collagen, MMP1, and its inhibitor TIMP1 did not differ between the A5-treated cells and the CTRL group (Fig. S2b). These results suggest that A5 has no direct impact on the regeneration of the extracellular matrix of dermal fibroblasts during wound healing.

3.8. A5 exerted complex regulation on endothelial cells

While our findings presented in Fig. 4 show that A5 treatment did not affect vascularization in diabetic wounds, we observed an interesting phenomenon in endothelial cells *in vitro*. In the CCK-8 assay, different concentrations of A5 exhibited no significant difference in the proliferation of HUVECs on days 1, 2, and 3 compared with the CTRL group (Fig. S3a). This implies that A5 had no direct effect on HUVEC proliferation. However, in the cell migration assay, compared to the 0-h scratch, the scratch of cells treated with A5 exhibited slight shrinkage at 12 h and more pronounced shrinkage at 24 h. The gap closure during the cell migration displayed a dose-dependent effect (Figs. S3b and c). These results indicated that A5 promoted the migration of HUVECs. In the tube formation assay, after 6 h of A5 treatment, the tubular structures formed by HUVECs decreased in a dose-dependent manner compared to those in the CTRL group (Fig. S3d), with a reduction in the mean tube length (Fig. S3e) and a decrease in branch points per mm^2 (Fig. S3f). This suggests that A5 inhibited HUVEC tube formation. Overall, these results indicated that in HUVECs, A5 promoted cell migration, had

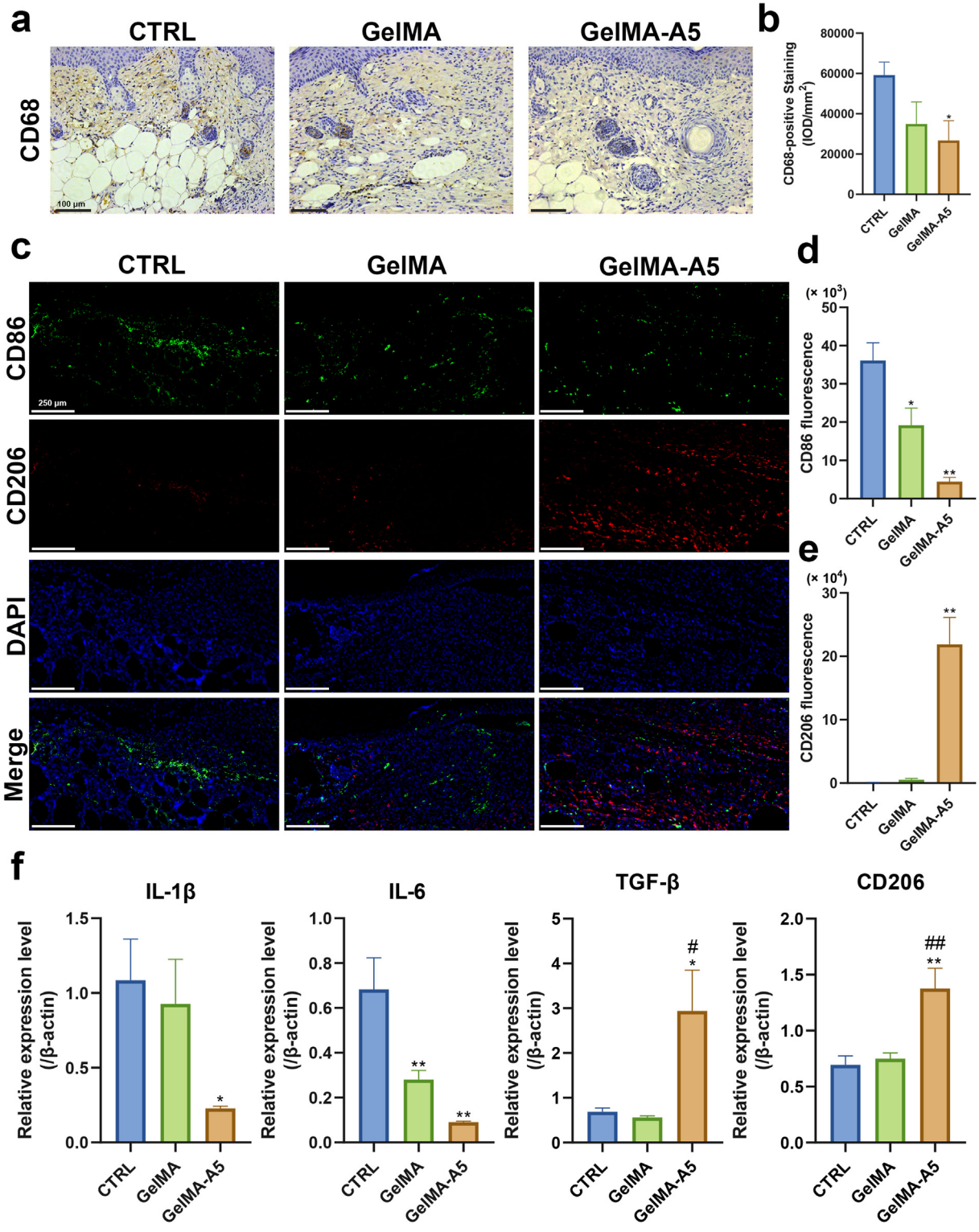

Fig. 3. The effect of A5 on regulating inflammation in diabetic wounds. A. Representative images of immunohistochemical anti-CD68 staining in diabetic wounds was performed. B. Quantitative analysis of integral optical density of anti-CD68-positive cell. C. Representative images of immunofluorescence anti-CD86 and anti-CD206 staining was performed. D&E. Quantitative analysis of fluorescence intensity of anti-CD86 and anti-CD206. F. Relative expression levels of IL-1β, IL-6, TGF-β and CD206 detected by qRT-PCR in diabetic wounds from the CTRL group, GelMA group, and GelMA-A5 group. Data are presented as mean ± SEM. Statistical analyses were performed by comparing the GelMA and GelMA-A5 groups to the CTRL group, where *p < 0.05, **p < 0.05; and by comparing the GelMA and GelMA-A5 groups, where #p < 0.05, ##p < 0.05.

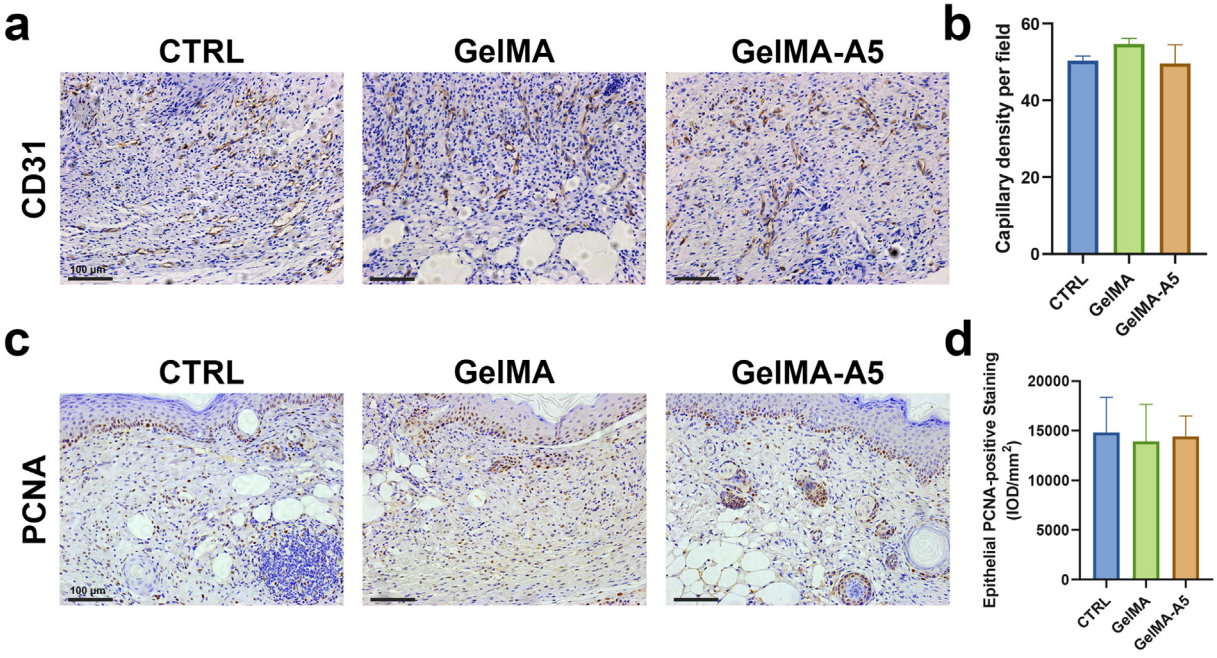

Fig. 4. The effect of A5 of angiogenesis and epithelial proliferation in diabetic wounds. A. Representative images of immunohistochemical anti-CD31 staining in diabetic wounds was performed. B. Quantitative analysis of capillary density of the number of anti-CD31-positive vessels. C. Representative images of immunohistochemical anti-PCNA staining in diabetic wounds was performed. D. Quantitative analysis of integral optical density of epithelial anti-PCNA-positive cell. Data are presented as mean ± SEM.

no effect on cell proliferation, and inhibited tube formation, which did not affect vascularization during wound healing *in vivo* (Fig. 4a).

4. Discussion

Diabetic wounds pose a significant challenge in terms of healing, primarily because of the persistent presence of chronic inflammation and ischemia, reduce cell proliferation and ECM secretion, and impaired epithelialization. These factors make wound healing difficult and prone to microbial infections, leading to a vicious cycle of inflammation-infection-inflammation [26]. In this study, we confirmed that topical application of a hydrogel loaded with A5 accelerated the healing of diabetic wounds. Detailed histological analysis revealed marked regulation of inflammation, effectively controlling active inflammation following A5 treatment. In *in vitro* experiments, we demonstrated that A5 could inhibit the activation of macrophages from the M0-phenotype to the M1-phenotype and promote the migration of epithelial cells. However, it has no direct impact on cell proliferation, tube formation by vascular endothelial cells, or ECM secretion by dermal fibroblasts. These findings suggested that A5 primarily promotes wound healing by regulating macrophage inflammation and by enhancing epithelialization.

Upon the occurrence of a common wound, immediate activation of hemostasis, such as blood vessel constriction and platelet activation, leads to the eventual formation of blood clots. Activated platelets release chemotactic factors that recruit inflammatory cells such as neutrophils and macrophages to adhere to the wound tissue [27]. Peripheral blood monocytes entering the wound area differentiate into macrophages, together with resident macrophages, with polarization from M0-phenotype macrophages to M1-phenotype macrophages [28]. M1-phenotype macrophages play a significant role in clearing pathogens, necrotic tissue, and apoptotic neutrophils, releasing pro-inflammatory cytokines (e.g., IL-1β, IL-6, and TNF-α), as well as growth factors (e.g., vascular endothelial growth factor and platelet derived growth factor) [29], and activating the transformation of dermal fibroblasts into myofibroblasts, and promoting cell migration and ECM secretion [30]. As the inflammatory response switches from M1-dominated to M2-dominated, the process of wound healing enters a phase of proliferation and regeneration [31]. M2-phenotype macrophages secrete anti-inflammatory cytokines (e.g., IL-4, IL-10, and IL-13) and growth factors (e.g., insulin-like growth factor 1 and TGF-β1), promoting epithelialization, ECM secretion, and angiogenesis [30]. In diabetic wounds, the transition of M1-phenotype macrophages to M2-phenotype macrophages is disrupted, leading to a prolonged microenvironment of oxidative stress, inadequate clearance of necrotic tissue, and active inflammation, thereby hindering the wound healing process [30]. Annexin A5, which is a novel anti-inflammatory protein, has a significant effect on inflammatory diseases, such as endotoxemia, inflammatory bowel disease, traumatic brain injury-induced intestinal injury and nonalcoholic steatohepatitis [32–35]. With traumatic brain injury, A5 treatment increased the ratio of M2/M1 phenotype microglia, with a reduction of IL-1β, IL-6 and iNOS and with an increasing in IL-10, by regulating the NF-kB/HMGB1 pathway and the Nrf2/HO-1 antioxidant system [36]. A5 has an effect on downregulation of pro-inflammatory factors (such as IL-1β, IL-6, and TNF-α) and upregulation of anti-inflammatory factors (such as CD206, Fizz1, and Ym1) and inhibition of the classical signaling pathways (STAT1, NF-κB, and MAPK) of macrophage polarization and induction of metabolic reprogramming of macrophages [35]. In this study, we observed that the wounds in diabetic mice remained unhealed on the 14th day (Fig. 1), and histological analysis indicated a lack of continuous epidermis in the wounds (Fig. 2), with notable infiltration of CD68-positive macrophages into the dermis (Fig. 3a), consistent with the characteristics of diabetic wounds. In the A5 treatment group, the diabetic wound tissues exhibited almost complete repair (Fig. 1) and histological analysis revealed an intact continuous epidermis, a clear and regular arrangement of collagen (Fig. 2), and a reduced number of $CD68^{+}$ cells in the dermis (Fig. 3a). The results of qRT-PCR revealed a decrease in the expressions of IL-1β and IL-6 from M1-phenotype macrophages in the A5 treatment group, while the

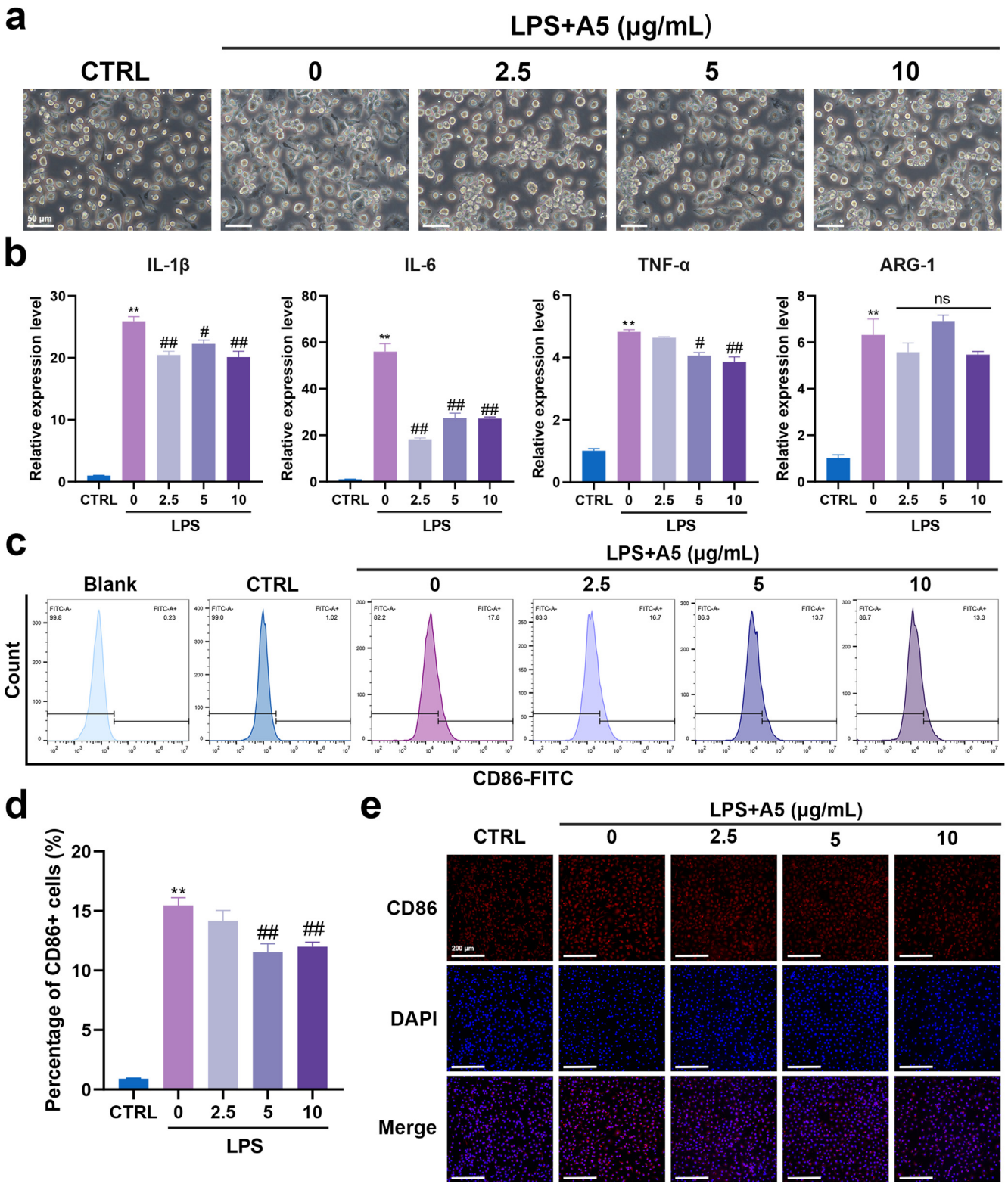

Fig. 5. A5 regulated LPS-stimulated inflammation of BMDMs. A. Morphology of LPS-stimulated primary macrophage BMDMs after 24 h of A5 treatment. B. Relative expression levels of IL-1β, IL-6, TNF-α and ARG-1 detected by qRT-PCR in LPS-stimulated BMDMs treated with A5 for 24 h. C&D. Percentages of $CD86^+$ cells of BMDMs after stimulated by LPS and treated with A5 detected by flow cytometry. E. Representative images of immunocytofluorescence anti-CD86 staining in LPS-stimulated BMDMs treated with A5. Data are presented as mean ± SEM. Statistical analyses were performed by comparing LPS+0 μg/mL A5 groups to the CTRL group, where *p < 0.05, **p < 0.05; and by comparing the LPS+2.5 μg/mL A5, +5 μg/mL A5 and +10 μg/mL A5 groups to LPS+0 μg/mL A5 group, where #p < 0.05, ##p < 0.05.

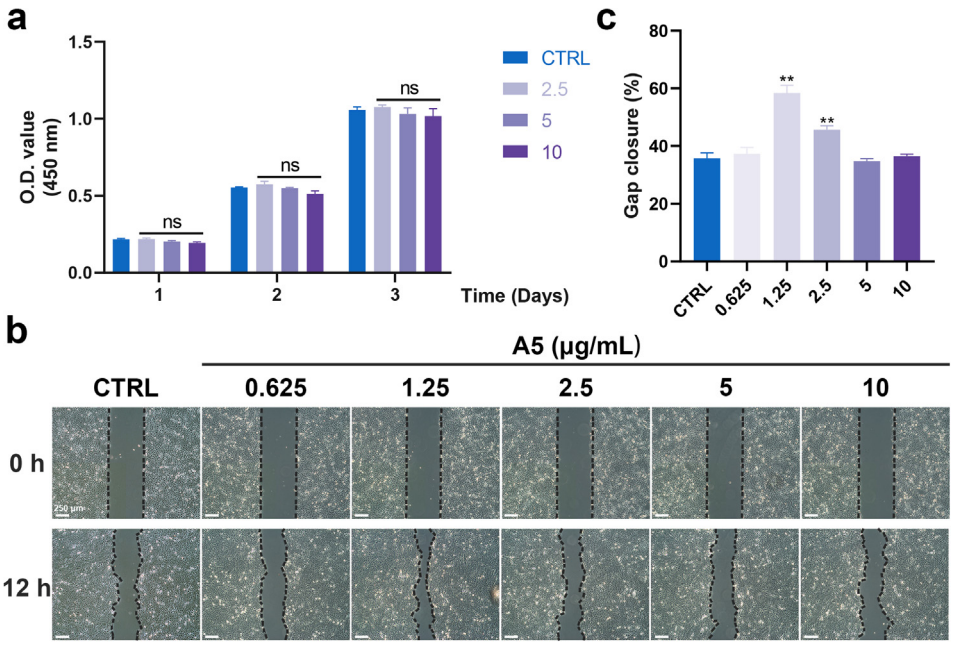

Fig. 6. A5 promoted cell migration of HaCaTs. A. A5 was co-cultured with HaCaTs at dose-dependent manner, and CCK-8 assays were conducted on days 1, 2, and 3. Experimental results are presented as the average absorbance at a wavelength of 450 nm ± SEM. B. Cell migration of HaCaTs treated with A5 was assessed through scratch assay at 0 and 12 h. C. Quantitative analysis of the percentage of gap closure (12 h). Data are presented as mean ± SEM. *p < 0.05, **p < 0.05.

expression of TGF-β and CD206 by M2-phenotype macrophages was increased. These results suggest that A5 inhibits the polarization of macrophages from the M0 to the M1 phenotype and promotes the shift of macrophages from the M1 to the M2 phenotype, leading to the regulation of inflammation and facilitation of diabetic wound healing into the phase of proliferation and tissue remodeling. The results of *in vitro* experiments also confirmed that A5 inhibited the polarization of macrophages from the M0 phenotype to the M1 phenotype (Fig. 5).

Epithelialization is a fundamental requirement during wound healing, with keratinocytes initiating this process several hours after wound occurrence and continuing until the wound is completely healed [37]. In chronic wounds, an active inflammatory microenvironment can lead to keratinocyte dysfunction, which is characterized by excessive proliferation but limited migration, resulting in hyperkeratosis and parakeratosis [38]. Previous studies have shown that A5 promotes epithelial cell migration and epithelialization without affecting their proliferation [39]. By increasing the release of urokinase-type plasminogen activators to promote epithelial cell migration, A5 accelerated corneal wound healing [40]. In the present study, we also confirmed *in vitro* that A5 had no effect on the proliferation of keratinocytes, but it enhanced their migration. This suggests that A5 accelerates epithelialization during the healing of diabetic wounds by promoting cell migration of keratinocytes. However, the specific mechanisms underlying these effects require further investigation.

The processes of cell proliferation and migration, along with the inflammatory response, require a substantial supply of oxygen and nutrients during wound healing. Therefore, it is commonly thought that sufficient vascularization is necessary to expedite wound healing [41]. In *in vivo* experiments, we did not observe any promotion of wound angiogenesis by A5 (Fig. 4a), and in *in vitro* experiments, we found that A5 promoted cell migration but had no effect on cell proliferation, and it inhibited tube formation of HUVECs (Fig. S3). This is consistent with earlier findings whereby A5 exhibited no biological effects on hepatic sinusoidal endothelial cells [35].

When comparing the effects of A5 treatment with those of CEFFE treatment in diabetic wounds, CEFFE achieved complete healing by the 14th day, whereas A5 treatment had not yet resulted in full healing. Under the CEFFE treatment, the key processes essential for diabetic wound healing were significantly promoted. CEFFE stimulated angiogenesis with higher capillary density, and regulated the infiltration of macrophage with reduced CD68-positive cells, and promoted the epithelization with enhanced proliferation and migration of epithelial cells [15]. In our research, we found that A5 treatment reduced the infiltration of macrophage, regulated the macrophage polarization from M1-phenotype to M2-phenotype, and promoted the migration of epithelial cells. These differences may be related to the diverse biological functions of bioactive proteins in CEFFE, such as their anti-inflammatory, pro-angiogenic, pro-proliferative, and antioxidant properties [42]. These results indicate that the primary biological effect of A5 is the regulation of macrophage-mediated inflammatory responses and epithelialization of keratinocytes. The regulation of inflammation and epithelialization is part of the process of wound healing. Future developments in medications for wound healing will need to explore combinations of various proteins with different biological functions to promote wound healing by regulating inflammation and promoting cell proliferation and angiogenesis, among other multi-target approaches.

Due to the suitable biocompatibility, biodegradability and anti-inflammatory property, GelMA hydrogels have emerged as a promising material for wound healing applications [43]. Our research findings, which demonstrate that GelMA-PBS hydrogels promoted diabetic wound healing and suppressed M1-phenotype inflammation in the GelMA group compared to the CTRL group (Figs. 1–3), are consistent with the known characteristics of GelMA. Moreover, GelMA hydrogels are known for their sustained drug release capabilities [43], which is essential for treating non-healing wounds, especially in regulating chronic inflammation. The drug release kinetics in GelMA hydrogels was investigated and fit best with Korsmeyer-Peppas model [44], which describe an initial burst release followed by sustained release [45]. Various compounds,

metallic ions, extracellular vesicles and exosomes loaded in GelMA have reached sustained release or controlled release in the drug delivery system [46–49]. Therefore, GelMA hydrogels hold great promise in the field of wound healing treatments.

Our study was based on the paracrine mechanisms of MSC and the effectiveness of CEFFE in the treatment of diabetic wounds. We identified crucial bioactive proteins and synthesized these proteins industrially using recombinant protein technology. This approach enables research on wound-healing biologics with clear molecular structures, well-defined mechanisms, controlled quality, and large-scale industrial production, thereby providing a new pathway for the development of stem cell-based regenerative medicine. The discovery of the anti-inflammatory protein A5 and its proven effectiveness in diabetic wound healing reaffirm the viability of this approach. In the future, we expect to see expansion of the application of A5 to the treatment of other diseases with inflammatory conditions, while also combining it with different proteins possessing various biological functions to address a broader range of clinically challenging diseases that require regenerative medicine solutions.

5. Conclusion

This research suggests that annexin A5 significantly accelerates diabetic wound healing by regulating macrophages inflammation by the transition of the M1-phenotype to the M2-phenotype, and epithelialization by the promotion of cell migration of keratinocyte. Since our research has shown the efficacy of annexin A5 in treating diabetic wounds, future studies are needed to determine the optimal concentration and regimen for clinical application. All in all, annexin A5 holds ample promise as an effective biological agent for the treatment of non-healing wounds.

Author contribution

The study was designed by W.L. and W.Z. B.K. and Z.J. contributed to experimentation, data collection, manuscript writing, editing, and data visualization. Y.D. carried out some of experiments. All authors read and approved the final manuscript.

Funding

This study was supported by the National Natural Science Foundation of China (81771993) the Shanghai Collaborative Innovation Program on Regenerative Medicine and Stem Cell Research (2019CXJQ01) (Shanghai, China). The funder had no role in data collection, management, analysis, publication decision, or manuscript preparation.

Data availability statement

The datasets during the current study are available from the corresponding author on reasonable request.

Declaration of competing interest

The author declares that they have no conflict of interest.

Appendix A. Supplementary data

Supplementary data to this article can be found online at https://doi.org/10.1016/j.reth.2024.03.013.

References

[1] Alavi A, Sibbald RG, Mayer D, Goodman L, Botros M, Armstrong DG, et al. Diabetic foot ulcers: Part I. Pathophysiology and prevention. J Am Acad Dermatol 2014;70(1 e1–18). quiz 19-20.
[2] Pierce GF. Inflammation in nonhealing diabetic wounds: the space-time continuum does matter. Am J Pathol 2001;159:399–403.
[3] Barrientos S, Stojadinovic O, Golinko MS, Brem H, Tomic-Canic M. Growth factors and cytokines in wound healing. Wound Repair Regen 2008;16:585–601.
[4] DiPietro LA. Wound healing: the role of the macrophage and other immune cells. Shock 1995;4:233–40.
[5] Brancato SK, Albina JE. Wound macrophages as key regulators of repair: origin, phenotype, and function. Am J Pathol 2011;178:19–25.
[6] Patel S, Maheshwari A, Chandra A. Biomarkers for wound healing and their evaluation. J Wound Care 2016;25:46–55.
[7] Zhao X, Chen J, Sun H, Zhang Y, Zou D. Correction: new insights into fibrosis from the ECM degradation perspective: the macrophage-MMP-ECM interaction. Cell Biosci 2022;12:138.
[8] Sen CK. Human wound and its burden: updated 2020 compendium of estimates. Adv Wound Care 2021;10:281–92.
[9] Yu X, Liu P, Li Z, Zhang Z. Function and mechanism of mesenchymal stem cells in the healing of diabetic foot wounds. Front Endocrinol 2023;14.
[10] Ouyang L, Qiu D, Fu X, Wu A, Yang P, Yang Z, et al. Overexpressing HPGDS in adipose-derived mesenchymal stem cells reduces inflammatory state and improves wound healing in type 2 diabetic mice. Stem Cell Res Ther 2022;13.
[11] Zhao H, Li Z, Wang Y, Zhou K, Li H, Bi S, et al. Bioengineered MSC-derived exosomes in skin wound repair and regeneration. Front Cell Dev Biol 2023;11.
[12] Park S-R, Kim J-W, Jun H-S, Roh JY, Lee H-Y, Hong I-S. Stem cell secretome and its effect on cellular mechanisms relevant to wound healing. Mol Ther 2018;26:606–17.
[13] De Gregorio C, Contador D, Díaz D, Cárcamo C, Santapau D, Lobos-Gonzalez L, et al. Human adipose-derived mesenchymal stem cell-conditioned medium ameliorates polyneuropathy and foot ulceration in diabetic BKS db/db mice. Stem Cell Res Ther 2020;11.
[14] Sell S. On the stem cell origin of cancer. Am J Pathol 2010;176:2584–94.
[15] Wang X, Deng M, Yu Z, Cai Y, Liu W, Zhou G, et al. Cell-free fat extract accelerates diabetic wound healing in db/db mice. Am J Transl Res 2020;12:4216–27.
[16] Yin M, Wang X, Yu Z, Wang Y, Wang X, Deng M, et al. gamma-PGA hydrogel loaded with cell-free fat extract promotes the healing of diabetic wounds. J Mater Chem B 2020;8:8395–404.
[17] Jia Z, Kang B, Cai Y, Chen C, Yu Z, Li W, et al. Cell-free fat extract attenuates osteoarthritis via chondrocytes regeneration and macrophages immunomodulation. Stem Cell Res Ther 2022;13:133.
[18] Raynal P, Pollard HB. Annexins: the problem of assessing the biological role for a gene family of multifunctional calcium- and phospholipid-binding proteins. Biochim Biophys Acta 1994;1197:63–93.
[19] Gerke V, Moss SE. Annexins: from structure to function. Physiol Rev 2002;82:331–71.
[20] Logue SE, Elgendy M, Martin SJ. Expression, purification and use of recombinant annexin V for the detection of apoptotic cells. Nat Protoc 2009;4:1383–95.
[21] Krahling S, Callahan MK, Williamson P, Schlegel RA. Exposure of phosphatidylserine is a general feature in the phagocytosis of apoptotic lymphocytes by macrophages. Cell Death Differ 1999;6:183–9.
[22] Tschirhart BJ, Lu X, Mokale Kognou AL, Martin CM, Slessarev M, Fraser DD, et al. Pharmacokinetics of recombinant human annexin A5 (SY-005) in patients with severe COVID-19. Front Pharmacol 2023;14:1299613.
[23] Martin CM, Slessarev M, Campbell E, Basmaji J, Ball I, Fraser DD, et al. Annexin A5 in patients with severe COVID-19 disease: a single-center, randomized, double-blind, placebo-controlled feasibility trial. Crit Care Explor 2023;5:e0986.
[24] Yue K, Trujillo-de Santiago G, Alvarez MM, Tamayol A, Annabi N, Khademhosseini A. Synthesis, properties, and biomedical applications of gelatin methacryloyl (GelMA) hydrogels. Biomaterials 2015;73:254–71.
[25] Dinh T, Veves A. Microcirculation of the diabetic foot. Curr Pharmaceut Des 2005;11:2301–9.
[26] Wilkinson HN, Hardman MJ. Wound healing: cellular mechanisms and pathological outcomes. Open Biol 2020;10:200223.
[27] Colvin BT. Physiology of haemostasis. Vox Sang 2004;87(Suppl1):43–6.
[28] Das A, Sinha M, Datta S, Abas M, Chaffee S, Sen CK, et al. Monocyte and macrophage plasticity in tissue repair and regeneration. Am J Pathol 2015;185:2596–606.
[29] Mahdavian Delavary B, van der Veer WM, van Egmond M, Niessen FB, Beelen RH. Macrophages in skin injury and repair. Immunobiology 2011;216:753–62.
[30] Hesketh M, Sahin KB, West ZE, Murray RZ. Macrophage phenotypes regulate scar formation and chronic wound healing. Int J Mol Sci 2017;18.
[31] Khallou-Laschet J, Varthaman A, Fornasa G, Compain C, Gaston AT, Clement M, et al. Macrophage plasticity in experimental atherosclerosis. PLoS One 2010;5:e8852.
[32] Arnold P, Lu X, Amirahmadi F, Brandl K, Arnold JM, Feng Q. Recombinant human annexin A5 inhibits proinflammatory response and improves cardiac

function and survival in mice with endotoxemia. Crit Care Med 2014;42:e32–41.
[33] Zhang X, Song L, Li L, Zhu B, Huo L, Hu Z, et al. Phosphatidylserine externalized on the colonic capillaries as a novel pharmacological target for IBD therapy. Signal Transduct Targeted Ther 2021;6:235.
[34] Zhang H, Gao Y, Li T, Li F, Peng R, Wang C, et al. Recombinant human annexin A5 alleviated traumatic-brain-injury induced intestinal injury by regulating the Nrf2/HO-1/HMGB1 pathway. Molecules 2022;27.
[35] Xu F, Guo M, Huang W, Feng L, Zhu J, Luo K, et al. Annexin A5 regulates hepatic macrophage polarization via directly targeting PKM2 and ameliorates NASH. Redox Biol 2020;36:101634.
[36] Gao Y, Zhang H, Wang J, Li F, Li X, Li T, et al. Annexin A5 ameliorates traumatic brain injury-induced neuroinflammation and neuronal ferroptosis by modulating the NF-κB/HMGB1 and Nrf2/HO-1 pathways. Int Immunopharm 2023;114:109619.
[37] Pastar I, Stojadinovic O, Yin NC, Ramirez H, Nusbaum AG, Sawaya A, et al. Epithelialization in wound healing: a comprehensive review. Adv Wound Care 2014;3:445–64.
[38] Stojadinovic O, Pastar I, Vukelic S, Mahoney MG, Brennan D, Krzyzanowska A, et al. Deregulation of keratinocyte differentiation and activation: a hallmark of venous ulcers. J Cell Mol Med 2008;12:2675–90.
[39] Nakao H, Watanabe M, Maki M. A new function of calphobindin I (annexin V). Promotion of both migration and urokinase-type plasminogen activator activity of normal human keratinocytes. Eur J Biochem 1994;223:901–8.
[40] Watanabe M, Kondo S, Mizuno K, Yano W, Nakao H, Hattori Y, et al. Promotion of corneal epithelial wound healing in vitro and in vivo by annexin A5. Invest Ophthalmol Vis Sci 2006;47:1862–8.
[41] Patel S, Srivastava S, Singh MR, Singh D. Mechanistic insight into diabetic wounds: pathogenesis, molecular targets and treatment strategies to pace wound healing. Biomed Pharmacother 2019;112.
[42] Yu Z, Cai Y, Deng M, Li D, Wang X, Zheng H, et al. Fat extract promotes angiogenesis in a murine model of limb ischemia: a novel cell-free therapeutic strategy. Stem Cell Res Ther 2018;9:294.
[43] Zhang J, Liu C, Li X, Liu Z, Zhang Z. Application of photo-crosslinkable gelatin methacryloyl in wound healing. Front Bioeng Biotechnol 2023;11:1303709.
[44] Khoshmaram K, Yazdian F, Pazhouhnia Z, Lotfibakhshaiesh N. Preparation and characterization of 3D bioprinted gelatin methacrylate hydrogel incorporated with curcumin loaded chitosan nanoparticles for in vivo wound healing application. Biomater Adv 2024;156:213677.
[45] Costa P, Sousa Lobo JM. Modeling and comparison of dissolution profiles. Eur J Pharmaceut Sci 2001;13:123–33.
[46] Zhu W, Dong Y, Xu P, Pan Q, Jia K, Jin P, et al. A composite hydrogel containing resveratrol-laden nanoparticles and platelet-derived extracellular vesicles promotes wound healing in diabetic mice. Acta Biomater 2022;154:212–30.
[47] Wang Y, Cao Z, Wei Q, Ma K, Hu W, Huang Q, et al. VH298-loaded extracellular vesicles released from gelatin methacryloyl hydrogel facilitate diabetic wound healing by HIF-1α-mediated enhancement of angiogenesis. Acta Biomater 2022;147:342–55.
[48] Hu N, Cai Z, Jiang X, Wang C, Tang T, Xu T, et al. Hypoxia-pretreated ADSC-derived exosome-embedded hydrogels promote angiogenesis and accelerate diabetic wound healing. Acta Biomater 2023;157:175–86.
[49] Sun Y, Liu X, Zhu Y, Han Y, Shen J, Bao B, et al. Tunable and controlled release of cobalt ions from metal-organic framework hydrogel nanocomposites enhances bone regeneration. ACS Appl Mater Interfaces 2021;13:59051–66.